Modeling of magneto-electric sensor using finite element method

Thu Trang Nguyen, Laurent Daniel, Frédéric Bouillault and Xavier Mininger

Laboratoire de Génie Electrique de Paris (LGEP)
CNRS (UMR8507), SUPELEC, UPMC, Univ Paris-Sud 11
11 Rue Joliot Curie, Plateau du Moulon
91192 Gif-sur-Yvette, France
prenom.nom@supelec.fr

ABSTRACT. *The purpose of this work is to model a magnetic field sensor based on magneto-electric effect. The magneto-electric effect is obtained by the combination of piezoelectric and magnetostrictive constituents in a multilayer. A non linear constitutive law of magnetostriction is developed in order to define the magnetostrictive coefficients of the magnetostrictive constituent under static magnetic field loading. A harmonic finite element calculation is then performed to study the response of the sensor. Indeed the magneto-electric coefficents of thesse devices are enhanced when a harmonic magnetic field is superimposed to the static field to measure.*

RÉSUMÉ. *Le but de ce travail est de modéliser un capteur de champ magnétique basé sur l'effet magnétoélectrique. L'effet magnéto-électrique est obtenu en combinant des constituants piézo-électriques et magnétostrictifs sous forme de multicouche. Afin de définir les coefficients magnétostrictifs du constituant magnétostrictif sous sollicitation magnétique statique, une loi de comportement magnétoélastique non linéaire est développée. Un calcul par éléments finis en régime harmonique est ensuite mis en œuvre de manière à étudier le comportement du capteur. Les coefficients magnétoélectriques de ces dispositifs sont en effet améliorés lorsqu'un champ magnétique alternatif est superposé au champ statique à mesurer.*

KEYWORDS: *magnetoelectric effect, magnetic field sensor, frequency effect*

MOTS-CLÉS : *effet magnetoélectrique, capteur de champ magnétique, modélisation harmonique*

Magnetic field sensors are one of the most widely used sensors due to their applications in the automotive, medical, aerospace, defense and computer industries. Currently, most of the magnetic field sensors are based on variable reluctance, Hall and magnetoresistive effects. A new technology allowing high-sensitivity and temperature-stability is to take advantage of magneto-electric (ME) effect in magnetostrictive/piezo-electric composite materials. The ME effect results from the combination of magnetostrictive effect and piezoelectric effect via elastic interaction.

This work deals with the numerical modelling of the response of a magnetic field sensor based on ME effect. The sensor studied in this paper has been developed and characterised by Dong and co-workers at the University of Technology of Hanoi, Vietnam. It is a tri-layer made of a piezoelectric layer between two magnetostrictive layers. For the practical measurement of a static magnetic field, a small harmonic magnetic field is imposed by the coil at mechanical resonance frequency of the sensor. This superimposition is known to enhance the magneto-electric coefficient. A harmonic electric voltage is therefore obtained between the electrodes of the piezoelectric layer.

The constitutive laws of each layer are first described. Piezoelectric constitutive law is assumed to be linear. The high non linearity of both magnetic and magnetostrictive behavior of the magnetostrictive layer is described and taken into account. These constitutive laws are then implemented into a 2D finite element formulation using the magnetic vector potential, the displacement and the electric voltage as unknowns of the problem.

The numerical problem is divided into two sub-problems. In a first part a static calculation is performed using the full non-linear constitutive laws in order to define the operating point corresponding to the intensity of the static magnetic field. The static magnetic induction can then be obtained and associated with the corresponding magnetostriction strain. This result is used to linearize the magnetic and magnetostrictive constitutive laws around the polarisation point. These linearised constitutive laws are then introduced into a harmonic calculation allowing the determination of the induced electric voltage at resonance frequency. The 2D finite element computation is performed according to several simplifying assumptions detailed in the paper.

A comparison between experimental and numerical results is given in terms of the complex shape of the electric voltage obtained as a function of the intensity of the applied static magnetic field. The proposed modelling approach is shown to capture the effects responsible for the ME response of magnetic field sensors made of magnetostrictive/piezoelectric composites, and open the way to ME sensors numerical optimisation.

1. Introduction

Magnetic field sensors are one of the most widely used sensors due to their applications in the automotive, medical, aerospace, defense and computer industries. Currently, most of the magnetic field sensors are based on variable reluctance,

Hall and magnetoresistive effects. A new technology allowing high-sensitivity and temperature-stability is to take advantage of magneto-electric (ME) effect in composite material (Fiebig, n.d.). The ME effect results from the combination of magnetostrictive effect and piezoelectric effect via elastic interaction. In order to optimize ME sensors, a numerical modeling is a valuable approach. Finite element models for Magneto-Electric effect can be found in the literature (Sunar *et al.*, n.d.; Liu *et al.*, n.d.; Biju *et al.*, n.d.). These models adapt to only linear case. The purpose of this work is to build a numerical model based on finite element method, accounting for the non-linearity of both magnetostrictive and magnetic behavior. Constitutive laws coupling mechanical/electric/magnetic effects are first described, and then introduced into the finite element formulation. A comparison to the experimental characterization of a ME sensor is then proposed.

2. Sensor Configuration

Figure 1 presents the configuration of a magnetic field sensor made at the University of Engineering and Technology in Hanoi, Vietnam (Giang *et al.*, n.d.). The magnetic field sensor based on ME materials exhibits an excellent ME coefficient up to 5.5 V/cm Oe, the resolution of sensor can be enhanced to 10^{-8}T (Dong *et al.*, (2006)). Using traditional Hall and magnetoresistive effects, the resolution obtained in commercial product is about 10^{-7}T. The sensor is a tri-layer consisting in a piezoelectric (pz) layer between two magnetostrictive (ms) layers. For the practical measurement of a static magnetic field, a harmonic magnetic field is imposed by the coil at mechanical resonance frequency of the sensor. This superimposition is known to enhance the magneto-electric coefficient (Bichurin *et al.*, n.d.). A harmonic electric voltage is therefore obtained between the electrodes of the piezoelectric layer.

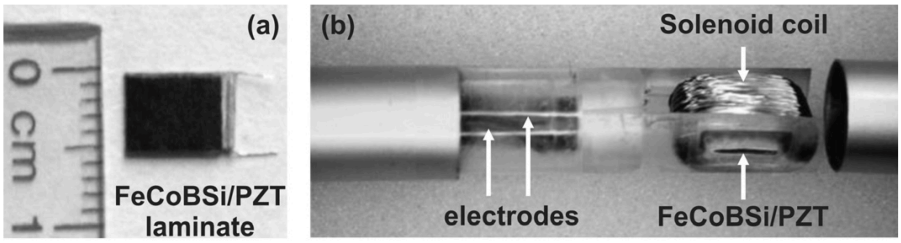

Figure 1: Magnetic field sensor based on ME effect

In a first study, the static and harmonic magnetic field are assumed to be along the same *x*-direction. The formulation uses the stress tensor $\mathbf{T}$, the strain tensor $\mathbf{S}$, the displacement $\mathbf{u}$, the driving force $\mathbf{f}$, the mass density ρ_m, the electric field $\mathbf{E}$, the electric flux density $\mathbf{D}$, the electrical voltage V, the charge density ρ, the magnetic field $\mathbf{H}$, the magnetic induction $\mathbf{B}$, the magnetic vector potential $\mathbf{a}$, the current density $\mathbf{J}$.

3. Equilibrium Equations

The mechanical equilibrium is given by:

$$\mathbf{div}\mathbf{T} + \mathbf{f} = \rho_m \frac{\partial^2 \mathbf{u}}{\partial t^2} \tag{1}$$

The electromagnetic equilibrium is given by:

$$\mathbf{curl}(\mathbf{H}) = \mathbf{J} \tag{2}$$

$$\mathrm{div}\mathbf{D} = \rho \tag{3}$$

No electric charge is considered ($\rho = 0$) in that case.

4. Constitutive Laws

4.1. Electroelastic Behavior

Considering that the piezoelectric is pre-polarized, the constitutive law is assumed to be linear around the polarization point:

$$\begin{pmatrix} \widetilde{\mathbf{T}} \\ \widetilde{\mathbf{D}} \end{pmatrix} = \begin{bmatrix} \widetilde{\mathbb{c}} & -\widetilde{\mathbb{e}}^{\mathrm{t}} \\ \widetilde{\mathbb{e}} & \widetilde{\mathbb{c}} \end{bmatrix}_{pz} \begin{pmatrix} \widetilde{\mathbf{S}} \\ \widetilde{\mathbf{E}} \end{pmatrix} \tag{4}$$

where $\widetilde{\mathbb{c}}$, $\widetilde{\mathbb{c}}$ and $\widetilde{\mathbb{e}}$ are respectively the stiffness tensor at constant electric field, the electric permittivity at constant strain and the piezoelectric coefficients. We note $\widetilde{X}(\widetilde{a}, \widetilde{b})$ the small variation of X around a polarization point $X_0(a_0, b_0)$:

$$\begin{aligned} X &= X_0 + \widetilde{X} \\ \widetilde{X} &= \frac{\partial X}{\partial a}(a_0, b_0)\widetilde{a} + \frac{\partial X}{\partial b}(a_0, b_0)\widetilde{b} \end{aligned} \tag{5}$$

4.2. Magnetostrictive Behavior

The polarization point of the magnetostrictive material is controlled by the static magnetic field $\mathrm{H_{dc}}$. Due to the non-linearity of magnetostriction, the corresponding constitutive law, depending on $\mathrm{H_{dc}}$, has to be investigated. The total stress $\mathbf{S}$ is divided into the elastic strain $\mathbf{S}^e$ and the magnetostriction strain $\mathbf{S}^\mu$, (Hirsinger *et al.*, n.d.): $s_{ij} = s^e_{ij} + s^\mu_{ij}$. Using Enstein's notation, the total stress can be calculated from Hooke's law:

$$t_{ij} = c^{ms}_{ijkl}(s_{kl} - s^\mu_{kl}) = c^{ms}_{ijkl}s_{kl} - t^\mu_{ij} \tag{6}$$

where c^{ms}_{ijkl} is the stiffness tensor of the material. In the case of an isotropic material, the Hooke law can be written in a simpler form using Lamé coefficient μ^* and λ^*:

$$\mathbf{T} = 2\mu^*\mathbf{S}^e + \lambda^*\mathrm{tr}(\mathbf{S}^e)\mathbb{I} \tag{7}$$

Equation (6) then becomes:

$$t_{ij} = 2\mu^*(s_{ij} - s^{\mu}_{ij}) + \delta_{ij}\lambda^*(s_{kk} - s^{\mu}_{kk}) \tag{8}$$

with s_{kk} the trace of $\mathbf{S}$ and δ_{ij} the Kronecker symbol. We assume that the magnetostriction phenomenon is isochoric and isotropic, and that the magnetostriction strain is a parabolic function of the magnetic polarization $\mathbf{M}$. Modifying the model of Galopin *et al.* (Galopin *et al.*, n.d.), that consider the magnetostriction strain as a parabolic function of the magnetic induction $\mathbf{B}$, and assuming that $\mathbf{B}$ and $\mathbf{M}$ are collinear, the strain can be expressed by:

$$s^{\mu}_{ij} = \frac{\beta}{2}(3b_ib_j - \delta_{ij}b_kb_k)\frac{m_pm_p}{b_pb_p} \tag{9}$$

where β is deduced from experimental measurements (Azoum *et al.*, n.d.). This expression will be used in order to calculate the terms $\dfrac{\partial t^{\mu}_{kl}}{b_i}$.
Using $\mathbf{S}$ and $\mathbf{B}$ as independent variables and following the thermodynamical approach of Besbes *et al.* (Besbes *et al.*, n.d.), the magnetic field can be expressed:

$$h_i = \nu_{ij}b_j - \frac{\partial t^{\mu}_{kl}}{\partial b_i}(s_{kl} - s^{\mu}_{kl}) \tag{10}$$

where ν_{ij} is the reluctivity tensor of the magnetostrictive material.

4.3. Linearized Form

The constitutive law of magnetostriction is strongly non linear. A static magnetic field $\mathrm{H_{dc}}$ imposes the magnetic polarization $\mathbf{M}_{\mathrm{dc}}$ and the magnetic induction $\mathbf{B}_{\mathrm{dc}}$, hence the polarization point. The constitutive law of magnetostriction around the polarization point can be calculated by differentiation of Equations (6) and (10), leading to the system (11):

$$\begin{aligned}
\widetilde{t}_{ij} &= c^{ms}_{ijkl}\widetilde{s}_{kl} - \frac{\partial t^{\mu}_{ij}}{\partial b_k}\widetilde{b}_k \\
\widetilde{h}_i &= -\frac{\partial t^{\mu}_{kl}}{\partial b_i}\widetilde{s}_{kl} + \left[\frac{\partial \nu_{ik}b_k}{\partial b_j} - \frac{\partial^2 t^{\mu}_{kl}}{\partial b_i \partial b_j}(s_{kl} - s^{\mu}_{kl}) + \frac{\partial t^{\mu}_{kl}}{\partial b_i}\frac{\partial s^{\mu}_{kl}}{\partial b_j}\right]\widetilde{b}_j
\end{aligned} \tag{11}$$

Considering free mechanical boundary conditions on the sensor and neglecting misfit strains, the term $s_{kl} - s^{\mu}_{kl}$ is assumed to be negligible. As a first approach the term $\dfrac{\partial t^{\mu}_{kl}}{\partial b_i}\dfrac{\partial s^{\mu}_{kl}}{\partial b_j}$ is considered negligible compared to the reluctivity of the magnetostrictive material. The system (11) can be simplified into:

$$\begin{aligned}
\widetilde{t}_{ij} &= c^{ms}_{ijkl}\widetilde{s}_{kl} - \frac{\partial t^{\mu}_{ij}}{\partial b_k}\widetilde{b}_k \\
\widetilde{h}_i &= -\frac{\partial t^{\mu}_{kl}}{\partial b_i}\widetilde{s}_{kl} - \nu_{ij}\widetilde{b}_j
\end{aligned} \tag{12}$$

As $s^{\mu}_{kk} = 0$ (isochoric magnetostriction), in the case of isotropic elasticity, from Equation (8), the term $\frac{\partial t^{\mu}_{kl}}{\partial b_i}$ can be written:

$$\frac{\partial t^{\mu}_{kl}}{\partial b_i} = 2\mu^* \frac{\partial s^{\mu}_{kl}}{\partial b_i} \tag{13}$$

and then:

$$\frac{\partial t^{\mu}_{kl}}{\partial b_i} = \mu^* \beta \left[\frac{\partial (3b_k b_l - \delta_{kl} b_j b_j)}{\partial b_i} \frac{m_p m_p}{b_q b_q} + (3b_k b_l - \delta_{kl} b_j b_j) \frac{\partial \frac{m_p m_p}{b_q b_q}}{\partial \sqrt{b_q b_q}} \frac{\partial b_t b_t}{\partial b_i} \right] \tag{14}$$

with

$$\frac{\partial b_t b_t}{\partial b_i} = \frac{b_i}{b_t b_t}$$

and

$$\frac{\partial (3b_k b_l - \delta_{kl} b_j b_j)}{\partial b_i} = \begin{cases} 4b_i & \text{if } k = l = i \\ -2b_i & \text{if } k = l \neq i \\ 3b_l & \text{if } k = i \neq l \\ 3b_k & \text{if } l = i \neq k \\ 0 & \text{else} \end{cases}$$

The non linear relationship between $\mathbf{M}$ and $\mathbf{H}$ is written using a Langevin type Equation (Bozorth, n.d.):

$$M = M_s (cotanh(A_s H M_s) - \frac{1}{A_s H M_s}) \tag{15}$$

with M_s the saturation magnetic polarization, A_s a constant that can be defined from the initial susceptibility χ_0 of the anhysteretic magnetization curve (Daniel *et al.*, n.d.): $A_s = \frac{3\mu_0 \chi_0}{M_s^2}$. Replacing in Equation (15) and using $B = \mu_0 H + M$, it comes:

$$B = \mu_0 H + M_s \left(\frac{1}{tanh(\frac{3\mu_0 \chi_0 H}{M_s})} - \frac{M_s}{3\mu_0 \chi_0 H} \right) \tag{16}$$

The terms $\frac{m_p m_p}{b_q b_q}$ and $\frac{\partial \frac{m_p m_p}{b_q b_q}}{\partial \sqrt{b_s b_s}}$ can be estimated numerically from Equation (16). For any polarization point, $\mathfrak{q}$ is the magnetostrictive tensor: $q_{kl} = \frac{t^{\mu}_{kl}}{\partial b_i}$. The constitutive law (13) can be expressed:

$$\begin{pmatrix} \widetilde{\mathbf{T}} \\ \widetilde{\mathbf{H}} \end{pmatrix} = \begin{bmatrix} \widetilde{\mathfrak{c}}^{ms} & -\widetilde{\mathfrak{q}}^{t} \\ -\widetilde{\mathfrak{q}} & \widetilde{\nu} \end{bmatrix} \begin{pmatrix} \widetilde{\mathbf{S}} \\ \widetilde{\mathbf{B}} \end{pmatrix} \tag{17}$$

5. Finite Element Formulation

5.1. Assumptions

5.1.1. Mechanical assumptions:

We consider a 2D problem with plane stress ($t_{31} = t_{32} = t_{33} = 0$) leading to the following relations:

$$\begin{cases} s^e_{31} = s^e_{32} = 0 \\ s^e_{33} = \dfrac{\lambda^*}{2\mu^* + \lambda^*}(s^e_{11} + s^e_{22}) \end{cases} \tag{18}$$

As s^e_{33} can be calculated afterwards, we only have to consider the mechanical variable in the working plane. In the finite element form, the mechanical variable chosen is the displacement $\mathbf{u}$ in the working plane:

$$s = \frac{1}{2}(\mathbf{grad}\mathbf{u} + \mathbf{grad}^t\mathbf{u}) = \mathcal{D}\mathbf{u} \tag{19}$$

5.1.2. Electromagnetic assumptions:

We consider a 2D problem with the following assumptions:

– No magnetic induction $\mathbf{B}$ nor electric field $\mathbf{E}$ are considered in the direction perpendicular to the working plane (z-direction). And $\mathbf{B}$ and $\mathbf{E}$ are assumed to be invariant with *z*.
We deduce:

– The magnetic vector potential is along *z*-direction and independent of z ($a_1 = a_2 = 0$).

– The electric field in the working plane $E_{/\!/}$ can be written: $E_{/\!/} = \mathbf{grad}V(x, y)$.
The electric voltage V and the magnetic vector potential along *z*-direction a_3 are chosen as the electromagnetic variables in the finite element formulation.

5.1.3. Finite Element Formulation

1) Mechanical Formulation: The mechanical formulation is established by taking into account the mechanical equilibrium (1) and the constitutive law deduced from Equation (4):

$$\mathbf{T} = \mathbb{c} : \mathbf{S} - \mathbb{e}^{\mathrm{t}}.\mathbf{E} - \mathbb{q}^{\mathrm{t}}.\mathbf{B}$$

Noting Ω the study domain, Γ_s its boundaries, the weak formulation of the mechanical equilibrium equation is:

$$\int_\Omega \mathbf{w}.\left(\mathrm{div}\mathbf{T} + \mathbf{f} - \rho_m \frac{\partial^2 \mathbf{u}}{\partial t^2}\right) d\Omega = 0 \tag{20}$$

where $\mathbf{w}$ is a vectorial test function.
Integrating by parts Equation (20) leads to:

$$\int_\Omega \left(\mathcal{D}\mathbf{w} : \mathbf{T} - \mathbf{w}.\mathbf{f} + \rho_m \mathbf{w}.\frac{\partial^2 \mathbf{u}}{\partial t^2}\right) d\Omega = \oint_{\Gamma_s} \mathbf{T}.\mathbf{n}.\mathbf{w}\, d\Gamma \tag{21}$$

with $\mathbf{n}$ the normal vector to the boundary Γ_s. The term on the right hand side of Equation (21) is related to the boundary conditions. There are two types of boundary conditions we need to contend with:

a) Dirichlet boundary condition: The values of $\mathbf{u}$ are known on a part of the boundary Γ_s.

b) Neumann condition: $\mathbf{T}.\mathbf{n} = 0$, the right hand side of Equation (21) is zero.

Replacing $\mathbf{S} = \mathcal{D}\mathbf{u}$, $\mathbf{E} = \mathbf{grad}V$ and $\mathbf{B} = \mathbf{curl}(\mathbf{a})$, Equation (21) can be written:

$$\begin{aligned}\int_\Omega \mathcal{D}\mathbf{w} : \mathbb{c} : \mathcal{D}\mathbf{u}\, d\Omega - \int_\omega \mathcal{D}\mathbf{w} : \mathbb{e}^t.\mathbf{grad}V\, d\Omega - \int_\Omega \mathcal{D}\mathbf{w} : \mathbb{q}^t.\mathbf{curl}(\mathbf{a})\, d\Omega \\ + \int_\Omega \rho_m \mathbf{w}\frac{\partial^2 \mathbf{u}}{\partial t^2}\, d\Omega = \int_\Omega \mathbf{w}.\mathbf{f} d\Omega + \oint_{\Gamma_s} \mathbf{T}.\mathbf{n}.\mathbf{w}\, d\Gamma\end{aligned} \tag{22}$$

In our mechanical problem no body force is considered ($\mathbf{f} = \mathbf{0}$).
The magnetic vector potential $\mathbf{a}$ is along *z*-direction, therefore: $\mathbf{curl}(\mathbf{a}) = \mathrm{r}^*\mathbf{grad}a_3$ with $\mathrm{r}^* = \begin{bmatrix} 0 & 1 \\ -1 & 0 \end{bmatrix}$.
In the finite element formulation, the displacement $\mathbf{u}$, the electric potential V, and the vector potential a_3 over an element are related to the corresponding node values $\{\mathbf{u}\}$, $\{V\}$ and $\{a_3\}$ using the shape functions $[\mathbf{w}]$, $[N_\mathrm{v}]$ and $[N_a]$:

$$\begin{aligned}\mathbf{u} &= [\mathbf{w}]\{\mathbf{u}\} \\ V &= [N_\mathrm{v}]\{V\} \\ a_3 &= [N_a]\{a_3\}\end{aligned} \tag{23}$$

Therefore the strain $\mathbf{S}$, the electrical field $\mathbf{E}$ and the magnetic induction $\mathbf{B}$ are associated to the nodal displacements and potentials by the derivatives $[G_u]$, $[G_\mathrm{v}]$ and $[G_a]$ of the shape functions:

$$\begin{aligned}\hat{\mathbf{S}} &= \mathcal{D}[\mathbf{w}]\{\mathbf{u}\} = [G_u]\{\mathbf{u}\} \\ \mathbf{E} &= \mathbf{grad}[N_\mathrm{v}]\{V\} = [G_\mathrm{v}]\{V\} \\ \mathbf{B} &= \mathrm{r}^*\mathbf{grad}[N_a]\{a_3\} = [\mathrm{r}^*][G_a]\{a_3\}\end{aligned} \tag{24}$$

After discretization Equation (22) can be written in the matrix form:

$$([\mathbb{K}_{uu}] - \omega^2[\mathbb{M}])\{\mathbf{u}\} + [\mathbb{K}_{up}]\{V\} + [\mathbb{K}_{ua}]\{a_3\} = [\mathbf{0}] \tag{25}$$

with,

$$\begin{aligned}[\mathbb{K}_{uu}] &= \sum_e \int_{\Omega^e} [G_u]^t[\hat{\mathbb{c}}][G_u]\, d\Omega \\ [\mathbb{M}] &= \sum_e \int_{\Omega^e} \rho_m[\mathbf{w}]^t[\mathbf{w}]\, d\Omega \\ [\mathbb{K}_{up}] &= -\sum_e \int_{\Omega^e} [G_u]^t[\hat{\mathbb{e}}^t][G_\mathrm{v}]\, d\Omega \\ [\mathbb{K}_{ua}] &= -\sum_e \int_{\Omega^e} [G_u]^t[\hat{\mathbb{q}}^t][\mathrm{r}^*][G_a]\, d\Omega\end{aligned} \tag{26}$$

Ω^e is the partial domain associated to the mesh element e. Equation (25) can be complemented with a damping term $j\omega\alpha[\mathbb{K}_{uu}]\{\mathbf{u}\}$ with α the damping coefficient. Noting $[\mathbb{K}^*_{uu}] = [\mathbb{K}_{uu}] + j\omega\alpha[\mathbb{K}_{uu}] - \omega^2[\mathbb{M}]$ gives:

$$[\mathbb{K}^*_{uu}]\{\mathbf{u}\} + [\mathbb{K}_{up}]\{V\} + [\mathbb{K}_{ua}]\{a_3\} = [\mathbf{0}] \tag{27}$$

2) Electromagnetic Formulation In a similar way, equations $\mathrm{div}\mathbf{D} = \rho$ and $\mathbf{curl}(\mathbf{H}) = \mathbf{J}$ gives the following expressions:

$$\begin{array}{l} [\mathbb{K}_{up}]^{\mathsf{t}}\{\mathbf{u}\} + [\mathbb{K}_{pp}]\{V\} = [Q] + [Q_n] \\ [\mathbb{K}_{ua}]^{\mathsf{t}}\{\mathbf{u}\} + [\mathbb{K}_{aa}]\{a_3\} = [I] + [I_n] \end{array} \tag{28}$$

with,

$$\begin{aligned} [\mathbb{K}_{pp}] &= \sum_e \int_{\Omega^e} [G_{\mathrm{v}}]^t [\mathfrak{c}] [G_{\mathrm{v}}]\, d\Omega \\ [Q] &= \sum_e \int_{\Omega^e} \rho [N_{\mathrm{v}}]^t\, d\Omega \\ [Q_n] &= \sum_e \oint_{\Gamma_s} D_n [N_{\mathrm{v}}]^t\, d\Gamma \\ [\mathbb{K}_{aa}] &= \sum_e \int_{\Omega^e} [G_a]^t [\mathfrak{r}^*]^t [\widetilde{\mathfrak{v}}] [\mathfrak{r}^*] [G_a]\, d\Omega \\ [I] &= \sum_e \int_{\Omega^e} j_3 [N_{\mathrm{v}}]^t\, d\Omega \\ [I_n] &= \sum_e \oint_{\Gamma_s} H_t [N_{\mathrm{v}}]^t\, d\Gamma \end{aligned} \tag{29}$$

$\widetilde{\mathfrak{v}}$ is the equivalent reluctivity tensor accounting for the magneto-elastic coupling (see section 4.3). D_n is the component of $\mathbf{D}$ normal to Γ_s, j_3 is the electric current along z-direction and H_t is the component of $\mathbf{H}$ tangent to Γ_s. In the case of the sensor studied in the following we will consider no electric charges ($\rho = 0$) and no current density (so that $j_3 = 0$). We finally obtain the system:

$$\begin{bmatrix} \mathbb{K}^*_{uu} & \mathbb{K}_{up} & \mathbb{K}_{ua} \\ \mathbb{K}_{pu} & \mathbb{K}_{pp} & \mathbb{0} \\ \mathbb{K}_{au} & \mathbb{0} & \mathbb{K}_{aa} \end{bmatrix} \left\{ \begin{array}{c} \mathbf{u} \\ V \\ a_3 \end{array} \right\} = \begin{bmatrix} \mathbf{0} \\ \mathbf{0} \\ I_n \end{bmatrix} \tag{30}$$

where $\mathbb{K}_{pu} = \mathbb{K}^{\mathsf{t}}_{up}$ describes the electro-mechanical coupling, $\mathbb{K}_{au} = \mathbb{K}^{\mathsf{t}}_{ua}$ describes the magneto-mechanical coupling. The linear system (30) is solved using Gauss algorithm.

5.1.4. Modeling Procedure

In order to calculate the electric voltage for any static magnetic field, the procedure is presented in Figure 2:

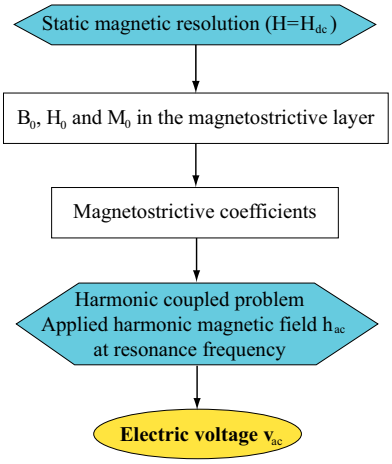

Figure 2: Modeling Procedure

6. Results

The purpose of this work is to reproduce qualitatively the results obtained for the ME sensor presented By Giang *et al.* (Giang *et al.*, n.d.). We focus on the numerical modeling of the sandwiched structure presented in Figure 3: The magnetostrictive material parameters correspond to those of Terfenol-D (Appendix 1) bonded with PZT (Appendix 2).

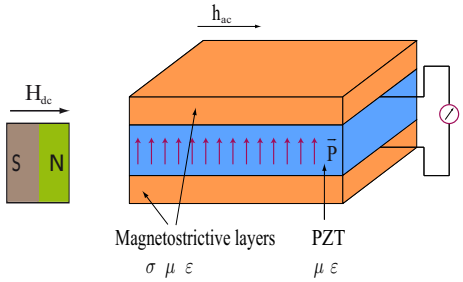

Figure 3: Structure of the magnetic field sensor

We first define the resonance frequency. Assuming no eddy current, the resonance frequency is the same as the mechanical resonance frequency: 73 kHz for the first

longitudinal mode. At this frequency, neglecting eddy current is appropriate because the skin depth calculated from analytical equation is much higher than the thickness of the magnetostrictive layers. The next step is to define the magnetostrictive coupling parameters for any H_{dc}. From Equation (14), the magnetostrictive coefficients can be defined if the magnetic induction $\mathbf{B}$, $\frac{m_p m_p}{b_q b_q}$ and $\frac{\partial \frac{m_p m_p}{b_q b_q}}{\partial \sqrt{b_s b_s}}$ are known. The first step is to solve a magnetic problem under static conditions. As the relationship between $\mathbf{B}$ and $\mathbf{H}$ is strongly non linear, the algebraic system obtained need to be solved by an iterative method. Figure 4 plots the variation of $\mathbf{B}$ in the magnetostrictive layers as a function of H_{dc}.

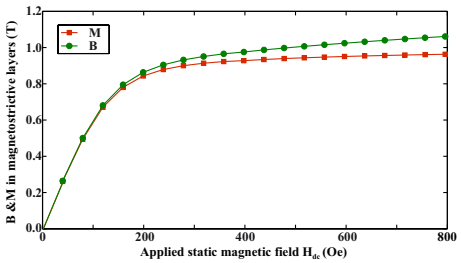

Figure 4: Magnetic induction and magnetic polarization in magnetostrictive layers versus applied static magnetic field

Figure 5 shows the experimental results obtained by D.T Huong Giang *et al.* (Giang *et al.*, n.d.) (circles). It plots the electric voltage between the electrodes of the piezoelectric layer as a function of the applied static magnetic field. The electric voltage first increases linearly and then decreases and approaches to 0. The ME coefficient depend on frequency of applied dynamic magnetic h_{ac}, it reach a maximum value under resonance frequency, a factor of 40 higher than under low frequency(Bichurin *et al.*, n.d.). The corresponding numerical result is shown in the same plot.

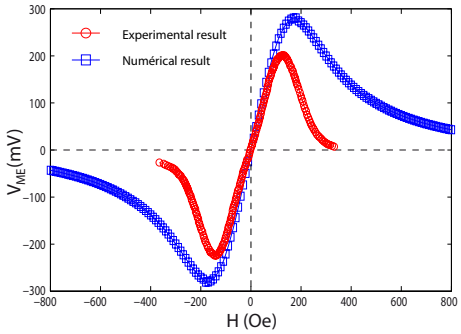

Figure 5: Experimental and numerical result: Electric voltage versus applied static magnetic field

For given piezoelectric coefficients, the electric voltage mainly depends on the magnetostrictive coefficients. From Figure 4, the magnetic polarization reaches a stable value while the magnetic induction still increases slightly. It leads to both $\frac{m_p m_p}{b_q b_q}$ and $\frac{\partial \frac{m_p m_p}{b_q b_q}}{\partial \sqrt{b_s b_s}}$ rapidly decreasing as the applied static magnetic field H_{dc} reaches high values. From Equations (12) and (14), the estimation of magnetostrictive coefficients being proportional to $\frac{m_p m_p}{b_q b_q}$ and $\frac{\partial \frac{m_p m_p}{b_q b_q}}{\partial \sqrt{b_s b_s}}$, one can expect that the magnetostrictive coefficients will first increase with H_{dc} and then decrease towards 0.
Figure 5 shows that the experimental and numerical results have a very similar shape. We can compare the result of electric voltage to the ones of magnetic induction and magnetic polarization obtained in Figure 4: The linear parts of the two curves are in the same range of applied magnetic field H_{dc}. A quantitative comparison would require a precise knowledge of specimen dimensions and material parameters. An experimental characterization to perform such a comparison is a work in progress.

7. Conclusion

In this paper, a numerical model using finite element method has been presented in order to describe the behavior of a magnetic field sensor based on magneto-electric effect. It makes use of a linear constitutive law for piezoelectric material and non linear constitutive law for magnetostrictive material. A specific linearization procedure around a pre-polarization point is proposed for the magnetostrictive material in order to investigate the effect of an additional harmonic magnetic field. This harmonic magnetic field is superimposed to the static field to be measured in order to obtain higher magnetoelectric conversion coefficients for the sensor. Numerical results are close to experimental measurements excerpted from the literature. Ongoing works concern the development of a 3D model.

Nomenclature:

$\mathbf{T}$	Stress tensor	$\mathbb{c}$	Stiffness tensor
$\mathbf{S}$	Strain tensor	$\mathbb{e}$	Piezoelectric tensor
$\mathbf{u}$	Mechanical displacement	$\mathbb{q}$	Magnetostrictive tensor
$\mathbf{f}$	Driving force	$\mathbb{c}$	Permittivity tensor
$\mathbf{E}$	Electric field	$\mathbb{\nu}$	Reluctivity tensor
$\mathbf{D}$	Electric flux density	μ^*, λ^*	Lamé elastic coefficients
$\mathbf{H}$	Magnetic field	χ_0	Initial susceptibility of anhysteretic magnetization curve
$\mathbf{B}$	Magnetic induction	μ	Magnetic permeability
$\mathbf{M}$	Magnetic polarization	$\mathbf{w}$	Vectorial test function
$\mathbf{J}$	Current density	β	Magnetostrictive coupling coefficient
$\mathbf{a}$	Magnetic vector potential	ρ	Charge density
V	Electric potential	ρ_m	Mass density

We note:

– $\widetilde{X}(\widetilde{a},\widetilde{b})$ the small variation of X around a polarization point $X_0(a_0,b_0)$:

$$X = X_0 + \widetilde{X}$$
$$\widetilde{X} = \frac{\partial X}{\partial a}(a_0,b_0)\widetilde{a} + \frac{\partial X}{\partial b}(a_0,b_0)\widetilde{b}$$

– x_i the component i of vector $\mathbf{X}$.

– x_{ij} the component ij of tensor $\mathbf{X}$.

Appendix 1:

Properties of magnetostrictive material

1) Stiffness tensor:

$$\begin{bmatrix} 1.24 & 0.61 & 0.61 & 0 & 0 & 0 \\ 0.61 & 1.42 & 0.61 & 0 & 0 & 0 \\ 0.61 & 0.61 & 1.42 & 0 & 0 & 0 \\ 0 & 0 & 0 & 0.54 & 0 & 0 \\ 0 & 0 & 0 & 0 & 0.54 & 0 \\ 0 & 0 & 0 & 0 & 0 & 0.63 \end{bmatrix} \times 10^{10} \text{ Pa}$$

2) Magnetic properties: $M_s = 1T \quad \chi_0 = 99$

3) Magnetostrictive parameter: $\beta = 5 \times 10^{-6}$

4) Density: 9200 kg/m^3

Appendix 2:

Properties of piezoelectric material

1) Stiffness tensor:

$$\begin{bmatrix} 3.19 & 1.43 & 1.43 & 0 & 0 & 0 \\ 1.43 & 3.19 & 1.43 & 0 & 0 & 0 \\ 1.43 & 1.43 & 2.67 & 0 & 0 & 0 \\ 0 & 0 & 0 & 0.68 & 0 & 0 \\ 0 & 0 & 0 & 0 & 0.58 & 0 \\ 0 & 0 & 0 & 0 & 0 & 0.58 \end{bmatrix} \times 10^{10} \text{ Pa}$$

2) Dielectric permittivity:

$$\begin{bmatrix} 15.92 & 0 & 0 \\ 0 & 15.92 & 0 \\ 0 & 0 & 15.92 \end{bmatrix} \times 10^{-9} \text{ A(s/Vm)}$$

3) Piezoelectric matrix:

$$\begin{bmatrix} 0 & -5.9 & 0 \\ 0 & -5.9 & 0 \\ 0 & 15.2 & 0 \\ 0 & 0 & 10.5 \\ 0 & 0 & 0 \\ 10.5 & 0 & 0 \end{bmatrix} \times \text{N/(Vm)}$$

4) Density: 7700 kg/m^3

References

Azoum K., Besbes M., Bouillault F., Ueno T.. (2006). Modeling of magnetostrictive phenomena. Application in magnetic force control, *IEEE Trans. Magn.*, n.d.

Besbes M., Ren Z., Razek A.. (2001). A generalized finite element model of magnetostriction phenomenas, *IEEE Trans. Magn.*, n.d.

Bichurin M. I., Filippov D. A., Petrov V. M., Laletsin V. M., Paddubnaya N., Srinivasan G.. (2003). Resonance magnetoelectric effects in layered magnetostrictive-piezoelectric composites, *Phys. Rev. B*, n.d.

Biju B., Ganesan N., Shankar K.. (2010). Finite element formulation using magnetic vector potential approach: effects of displacement current in magneto-electro-elastic cylindrical shells, *Smart Materials and Structures*, n.d.

Bozorth R.. *(1951). Ferromagnetism*, Van Nostrand, Princeton, NJ., n.d.

Daniel L., Hubert O., Buiron N., Billardon R.. (2008). Reversible magneto-elastic behavior: A multiscale approach, *J. Mech. Phys. Sol.*, n.d.

Dong S., Li J.-F., Viehland D.. (2006). Small dc magnetic field response of magnetoelectric laminate composites, *Applied Physics Letters*, (2006).

Fiebig M.. (2005). Revival of the magnetoelectric effect, *Journal Physics D: Applied Physics*, n.d.

Galopin N., Mininger X., Bouillault F., Daniel L.. (2008). Finite element modeling of magnetoelectric sensors, *IEEE Trans. Magn.*, n.d.

Giang D. T. H., Duc N. H.. (2009). Magnetoelectric sensor for microtesla magnetic-fields based on (Fe80Co20)78Si12B10/PZT laminates, *Sensors and Actuators A.*, n.d.

Hirsinger L., Billardon R.. (1995). Magneto-elastic finite element analysis including magnetic forces and magnetostriction effects, *IEEE Trans. Magn.*, n.d.

Liu Y. X., Wan J. G., Liu J. M., Nan C. W.. (2003). Numerical modeling of magnetoelectric effect in a composite structure, *J. Appl. Phys.*, n.d.

Sunar M., Al-Garni A. Z., Ali M. H., Kahraman R.. (2002). Finite Element Modeling of Thermopiezomagnetic Smart Structures, *AIAA Journal*, n.d.